Article

Protonation and Reactivity towards Carbon Dioxide of the Mononuclear Tetrahedral Zinc and Cobalt Hydroxide Complexes, [Tp$^{Bu^t}$]ZnOH and [Tp$^{Bu^t}$]CoOH: Comparison of the Reactivity of the Metal Hydroxide Function in Synthetic Analogues of Carbonic Anhydrase

Catherine Bergquist, Tauqir Fillebeen, Melissa M. Morlok, and Gerard Parkin

J. Am. Chem. Soc., **2003**, 125 (20), 6189-6199• DOI: 10.1021/ja034711j • Publication Date (Web): 29 April 2003

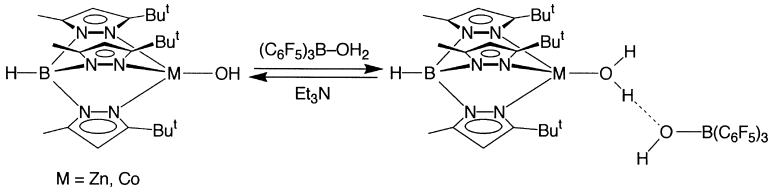

More About This Article

Additional resources and features associated with this article are available within the HTML version:

- Supporting Information
- Links to the 15 articles that cite this article, as of the time of this article download
- Access to high resolution figures
- Links to articles and content related to this article
- Copyright permission to reproduce figures and/or text from this article

View the Full Text HTML

J|A|C|S
ARTICLES
Published on Web 04/29/2003

Protonation and Reactivity towards Carbon Dioxide of the Mononuclear Tetrahedral Zinc and Cobalt Hydroxide Complexes, [Tp^{But,Me}]ZnOH and [Tp^{But,Me}]CoOH: Comparison of the Reactivity of the Metal Hydroxide Function in Synthetic Analogues of Carbonic Anhydrase

Catherine Bergquist, Tauqir Fillebeen, Melissa M. Morlok, and Gerard Parkin*

Contribution from the Department of Chemistry, Columbia University, New York, New York 10027

Received February 17, 2003; E-mail: parkin@chem.columbia.edu

Abstract: The tris(3-*tert*-butyl-5-methylpyrazolyl)hydroborato zinc hydroxide complex [Tp^{But,Me}]ZnOH is protonated by $(C_6F_5)_3B(OH_2)$ to yield the aqua derivative $\{[Tp^{But,Me}]Zn(OH_2)\}[HOB(C_6F_5)_3]$, which has been structurally characterized by X-ray diffraction, thereby demonstrating that protonation results in a lengthening of the Zn−O bond by ca. 0.1 Å. The protonation is reversible, and treatment of $\{[Tp^{But,Me}]Zn(OH_2)\}^+$ with Et_3N regenerates [Tp^{But,Me}]ZnOH. Consistent with the notion that the catalytic hydration of CO_2 by carbonic anhydrase requires deprotonation of the coordinated water molecule, $\{[Tp^{But,Me}]Zn(OH_2)\}^+$ is inert towards CO_2, whereas [Tp^{But,Me}]ZnOH is in rapid equilibrium with the bicarbonate complex [Tp^{But,Me}]ZnOC(O)OH under comparable conditions. The cobalt hydroxide complex [Tp^{But,Me}]CoOH is likewise protonated by $(C_6F_5)_3B(OH_2)$ to yield the aqua derivative $\{[Tp^{But,Me}]Co(OH_2)\}[HOB(C_6F_5)_3]$, which is isostructural with the zinc complex. The aqua complexes $\{[Tp^{But,Me}]M(OH_2)\}[HOB(C_6F_5)_3]$ (M = Zn, Co) exhibit a hydrogen bonding interaction between the metal aqua and boron hydroxide moieties. This hydrogen bonding interaction may be viewed as analogous to that between the aqua ligand and Thr-199 at the active site of carbonic anhydrase. In addition to the structural similarities between the zinc and cobalt complexes, [Tp^{But,Me}ZnOH] and [Tp^{But,Me}]-CoOH, and between $\{[Tp^{But,Me}]Zn(OH_2)\}^+$ and $\{[Tp^{But,Me}]Co(OH_2)\}^+$, DFT (B3LYP) calculations demonstrate that the pK_a value of $\{[Tp]Zn(OH_2)\}^+$ is similar to that of $\{[Tp]Co(OH_2)\}^+$. These similarities are in accord with the observation that Co^{II} is a successful substitute for Zn^{II} in carbonic anhydrase. The cobalt hydroxide [Tp^{But,Me}]CoOH reacts with CO_2 to give the bridging carbonate complex $\{[Tp^{But,Me}]Co\}_2(\mu\text{-}\eta^1,\eta^2\text{-}CO_3)$. The coordination mode of the carbonate ligand in this complex, which is bidentate to one cobalt center and unidentate to the other, is in contrast to that in the zinc counterpart $\{[Tp^{But,Me}]Zn\}_2(\mu\text{-}\eta^1,\eta^1\text{-}CO_3)$, which bridges in a unidentate manner to both zinc centers. This difference in coordination modes concurs with the suggestion that a possible reason for the lower activity of Co^{II}−carbonic anhydrase is associated with enhanced bidentate coordination of bicarbonate inhibiting its displacement.

Introduction

Zinc plays an essential role in biological systems, primarily via its function in more than ca. 300 enzymes.[1] However, as a result of the poor spectroscopic properties associated with the Zn^{II} ion, it is a nontrivial issue to determine the structure of the active site of a zinc enzyme in solution; correspondingly, it is difficult to determine the fine details of the mechanism of action of a zinc enzyme. To circumvent the problems resulting from the poor spectroscopic properties of Zn^{II}, metal-substituted zinc enzymes have been widely investigated.[2,3] For example, substitution of Zn^{II} by Co^{II} and Cd^{II} enables the enzyme systems to be probed by UV−visible and NMR spectroscopy, respectively.[4] However, the ability to use metal ion substitution to provide insight into the structures and mechanisms of action of the native zinc enzymes depends critically on knowledge of the chemistry of the pertinent metal ions in coordination environ-

(1) (a) Vallee, B. L.; Auld, D. S. *Acc. Chem. Res.* **1993**, *26*, 543−551. (b) Auld, D. S. *Structure and Bonding*; Springer-Verlag: New York, 1997; Vol. 89, pp 29−50. (c) Coleman, J. E. *Curr. Opin. Chem. Biol.* **1998**, *2*, 222−234. (d) Holm, R. H.; Kennepohl, P.; Solomon, E. I. *Chem. Rev.* **1996**, *96*, 2239−2314. (e) Lipscomb, W. N.; Sträter, N. *Chem. Rev.* **1996**, *96*, 2375−2433. (f) Lindskog, S. *Pharmacol. Ther.* **1997**, *74*, 1−20.

(2) For a general review of the application of cobalt as a probe and label of proteins, see: Maret, W.; Vallee, B. L. *Methods Enzymol.* **1993**, *226*, 52−71.

(3) For some studies on Co^{II}−carbonic anhydrase, see: (a) Banci, L.; Bertini, I.; Luchinat, C.; Donaire, A.; Martinez, M. J.; Moratal Mascarell, J. M. *Comments Inorg. Chem.* **1990**, *9*, 245−261. (b) Bertini, I.; Luchinat, C. *Acc. Chem. Res.* **1983**, *16*, 272−279. (c) Bertini, I.; Lanini, G.; Luchinat, C. *J. Am. Chem. Soc.* **1983**, *105*, 5116−5118. (d) Khalifah, R. G.; Rogers, J. I.; Harmon, P.; Morely, P. J.; Carroll, S. B. *Biochemistry* **1984**, *23*, 3129−3136. (e) Briganti, F.; Pierattelli, R.; Scozzafava, A.; Supuran, C. T. *Eur. J. Med. Chem.* **1996**, *31*, 1001−1010. (f) Bertini, I.; Luchinat, C.; Pierattelli, R.; Vila, A. J. *Eur. J. Biochem.* **1992**, *208*, 607−615. (g) Bertini, I.; Luchinat, C.; Pierattelli, R.; Vila, A. J. *Inorg. Chem.* **1992**, *31*, 3975−3979. (h) Håkansson, K.; Wehnert, A. *J. Mol. Biol.* **1992**, *228*, 1212−1218.

(4) Only recently have investigations using ^{67}Zn NMR spectroscopy in biological and related systems become feasible. See: (a) Lipton, A. S.; Bergquist, C.; Parkin, G.; Ellis, P. D. *J. Am. Chem. Soc.* **2003**, *125*, 3768−3772. (b) Lipton, A. S.; Buchko, G. W.; Sears, J. A.; Kennedy, M. A.; Ellis, P. D. *J. Am. Chem. Soc.* **2001**, *123*, 992−993.

ments that are relevant to those of enzyme active sites.[5] For this reason, studies of synthetic analogues (i.e., small molecules that resemble the enzyme active sites)[5,6] and their various metal substituted derivatives are of particular value. However, there are presently no experimental reports that compare directly the reactivity of the terminal Zn−OH entity with other M−OH groups in coordination environments that mimic enzyme active sites, despite the fact that the Zn−OH functionality is central to the mechanisms of action of many zinc enzymes.[1] Prompted by the lack of such studies, we compare here the chemistry of isostructural monomeric tetrahedral terminal hydroxide complexes of zinc and cobalt that are relevant to zinc enzymes. This investigation includes (i) the synthesis and structural characterization of the first pair of zinc and cobalt aqua complexes to be obtained by protonation of the hydroxide form of synthetic analogues of Zn^{II} and Co^{II}−carbonic anhydrases, and (ii) the demonstration that such protonation inhibits reactivity towards CO_2. These studies extend our initial report concerned with the structure and reactivity of the zinc complex $\{[Tp^{Bu^t,Me}]Zn(OH_2)\}^+$.[7]

Results and Discussion

The $[(His)_3Zn^{II}(OH_n)]$ ($n = 1, 2$) motif, which features a tetrahedral zinc center coordinated to the nitrogen atoms of three histidine imidazole groups and a water molecule or hydroxide ligand, is common to the active sites of a variety of zinc enzymes, including carbonic anhydrase, dihydroorotase, matrix metalloproteinases, and adamalysin II.[1] As a result, considerable effort has been directed towards isolating synthetic analogues that portray the $\{[NNN]ZnOH_n\}$ coordination environment. Particularly noteworthy examples are provided by the following complexes, each of which features a mononuclear tetrahedral center with either a hydroxide or an aqua ligand: $[Tp^{Bu^t,Me}]ZnOH$,[8] $[Tp^{Ar,Me}]ZnOH$ ($Ar = C_6H_4Pr^i$),[9] $\{[Pim^{Pr^i,Bu^t}]ZnOH\}(ClO_4)$,[10] and $[(X_6Et_3Imet_3)Zn(OH_2)\cdot(OH_2)]^{2+}$, where $X_6Et_3Imet_3$ is a calixarene-based ligand that possesses three imidazole donors.[11] By comparison to these zinc complexes, there has been less success in synthesizing structurally analogous complexes for other metals because a different type of structure often results. For example, whereas $\{[Pim^{Pr^i,Bu^t}]ZnOH\}^+$ exists as a tetrahedral hydroxide complex,[10] the cadmium counterpart $\{[Pim^{Pr^i,Bu^t}]Cd(OH_2)(OClO_3)\}^+$ exists as a five-coordinate complex with an aqua ligand.[12] Likewise, whereas $[Tp^{Pr^i_2}]ZnOH$ exists as a tetrahedral terminal hydroxide derivative, the manganese, iron, cobalt, nickel, and copper derivatives exist as five-coordinate dinuclear complexes with bridging hydroxide ligands, $\{[Tp^{Pr^i_2}]M(\mu\text{-}OH)\}_2$ (M = Mn, Fe, Co, Ni, Cu).[13] To our knowledge, the only pair of structurally related tetrahedral zinc and cobalt hydroxide complexes of the type $\{[N_3]MOH\}$ are the tris(pyrazolyl)hydroborato derivatives $[Tp^{Bu^t,Me}]ZnOH$[8] and $[Tp^{Bu^t,Me}]CoOH$.[14] For this reason, $[Tp^{Bu^t,Me}]ZnOH$ and $[Tp^{Bu^t,Me}]CoOH$ form the basis of the present investigation.

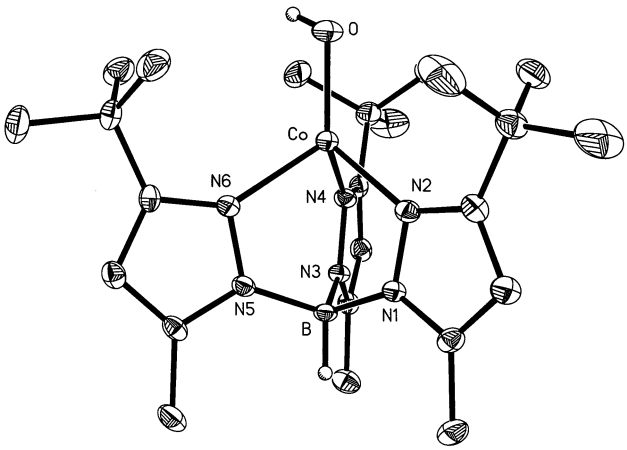

Figure 1. Molecular structure of $[Tp^{Bu^t,Me}]CoOH$. Selected bond lengths (Å): Co−O, 1.859(3); Co−N(2), 2.051(3); Co−N(4), 2.033(3); Co−N(6), 2.046(3).

(a) Structural Comparison of $[Tp^{Bu^t,Me}]ZnOH$ and $[Tp^{Bu^t,Me}]CoOH$. A comparison of structurally related zinc and cobalt hydroxide compounds is particularly relevant in view of the fact that cobalt is one of the metals for which activity is maintained.[2,3,15] In this regard, although the cobalt complex $[Tp^{Bu^t,Me}]CoOH$ was formulated as a mononuclear species,[14] its structure as determined by X-ray diffraction has not been reported. Since the closely related derivative $\{[Tp^{Pr^i_2}]Co(\mu\text{-}OH)\}_2$ has been shown to be a dimer,[13] we viewed it essential at the outset to determine the structure of $[Tp^{Bu^t,Me}]CoOH$ to (i) confirm its mononuclear nature and (ii) provide a detailed structural comparison with the zinc complex $[Tp^{Bu^t,Me}]ZnOH$. The molecular structure of $[Tp^{Bu^t,Me}]CoOH$ was, therefore, determined by X-ray diffraction (Figure 1), thereby verifying its monomeric nature. Thus, whereas the isopropyl substituents of the $[Tp^{Pr^i_2}]$ ligand are incapable of preventing the hydroxide ligand from bridging and forming the dimer $\{[Tp^{Pr^i_2}]Co(\mu\text{-}OH)\}_2$, the steric demands of the *tert*-butyl groups are sufficient to maintain a monomeric structure for $[Tp^{Bu^t,Me}]CoOH$ with a terminal hydroxide ligand. The X-ray diffraction study also indicates that the zinc and cobalt complexes have very similar coordination environments, as illustrated by comparison of their respective M−O and M−N bond lengths: Zn−O [1.850(8) Å][8] and Co−O [1.859(3) Å]; $Zn-N_{av}$ (2.10 Å)[8] and Co−N (2.04 Å). The Co−O bond length in $[Tp^{Bu^t,Me}]CoOH$ [1.859(3) Å] is also similar to that in five-coordinate $\{[P(CH_2CH_2PPh_2)_3]CoOH\}^+$ [1.873(7) Å];[16] these Co−OH bond lengths are, however, considerably shorter than that in the five-coordinate anionic species $\{[\eta^4\text{-}N\{CH_2CH_2NC(O)NHBu^t\}_3]CoOH\}^{2-}$ [2.052(3) Å], presumably due to the fact that hydroxide oxygen in the latter complex is also a hydrogen bond receptor for two of the urea substituents.[17]

(5) (a) Parkin, G. In *Met. Ions Biol. Syst*; Sigel, A., Sigel, H., Eds.; M. Dekker: New York, 2001; Vol. 38, Chapter 14, pp 411−460. (b) Parkin, G. *Chem. Commun.* **2000**, 1971−1985.
(6) (a) Kimura, E.; Kikuta, E. *J. Biol. Inorg. Chem.* **2000**, *5*, 139−155. (b) Vahrenkamp, H. *Acc. Chem. Res.* **1999**, *32*, 589−596.
(7) Bergquist, C.; Parkin, G. *J. Am. Chem. Soc.* **1999**, *121*, 6322−6323.
(8) Alsfasser, R.; Trofimenko, S.; Looney, A.; Parkin, G.; Vahrenkamp, H. *Inorg. Chem.* **1991**, *30*, 4098−4100.
(9) Ruf, M.; Vahrenkamp, H. *Inorg. Chem.* **1996**, *35*, 6571−6578.
(10) Kimblin, C.; Allen, W. E.; Parkin, G. *J. Chem. Soc., Chem. Commun.* **1995**, 1813−1815.
(11) Sénèque, O.; Rager, M.-N.; Giorgi, M.; Reinaud, O. *J. Am. Chem. Soc.* **2001**, *123*, 8442−8443.
(12) Kimblin, C.; Parkin, G. *Inorg. Chem.* **1996**, *35*, 6912−6913.
(13) Kitajima, N.; Hikichi, S.; Tanaka, M.; Moro-oka, Y. *J. Am. Chem. Soc.* **1993**, *115*, 5496−5508.
(14) Egan, J. W.; Haggerty, B. S.; Rheingold, A. L.; Sendlinger, S. C.; Theopold, K. H. *J. Am. Chem. Soc.* **1990**, *112*, 2445−2446.
(15) Lindskog, S.; Malmström, B. G. *J. Biol. Chem.* **1962**, *237*, 1129−1137.
(16) Orlandini, A.; Sacconi, L. *Inorg. Chem.* **1976**, *15*, 78−85.
(17) MacBeth, C. E.; Hammes, B. S.; Young, V. G.; Borovik, A. S. *Inorg. Chem.* **2001**, *40*, 4733−4741.

Scheme 1

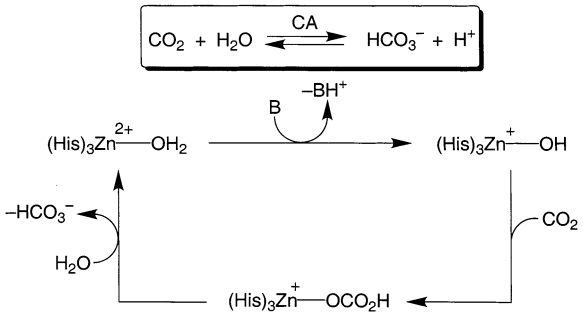

Scheme 2

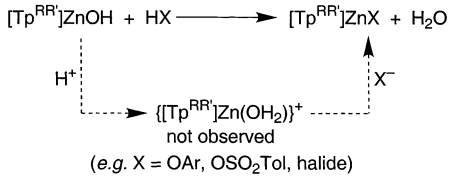

(b) Protonation of the Hydroxide Ligands in [Tp$^{Bu^t,Me}$]-ZnOH and [Tp$^{Bu^t,Me}$]CoOH: Synthesis and Structural Characterization of the Aqua Complexes {[Tp$^{Bu^t,Me}$]Zn-(OH$_2$)}[HOB(C$_6$F$_5$)$_3$] and {[Tp$^{Bu^t,Me}$]Co(OH$_2$)}[HOB(C$_6$F$_5$)$_3$]. Reversible proton transfer, which serves to interconvert the aqua and hydroxide forms of the active sites, $[Zn-OH_2]^{2+}$ and $[Zn-OH]^{+}$, is an essential step in the catalytic cycle of many zinc enzymes, such as carbonic anhydrase (Scheme 1).[1] It is, therefore, perhaps surprising that a well-defined example of this interconversion is unknown for a synthetic analogue system in which both partners have been isolated and structurally characterized. The absence of such a report is not a result of the systems studied being inert to proton transfer, but is rather a consequence of subsequent reactivity resulting in degradation. For example, protonation of the hydroxide ligand in [Tp$^{RR'}$]-ZnOH derivatives is facile, but the incipient aqua ligand is typically irreversibly displaced by the counterion (Scheme 2).[18] As an illustration, [Tp$^{Bu^t,Me}$]ZnOH reacts with *p*-TolS(O)$_2$OH to give [Tp$^{Bu^t,Me}$]ZnOS(O)$_2$Tol.[18c]

In view of the facile formation of [Tp$^{RR'}$]ZnX complexes in reactions of [Tp$^{RR'}$]ZnOH with simple acids, we sought for alternative acids, the counterion of which would not displace the coordinated water molecule. Previous studies have reported that treatment of both [Tp$^{Bu^t,Me}$]ZnOH and [Tp^{Cum,Me}]ZnOH with $HClO_4$ results in hydrolytic destruction of the tris(pyrazolyl)-borato ligand.[18c] In view of this type of degradation employing $HClO_4$, we thought it appropriate to investigate the application of anhydrous acids, such as $[H(OEt_2)_2][B(Ar_F)_4]$ (Ar_F = 3,5-$(CF_3)_2C_6H_3$). However, treatment of [Tp$^{Bu^t,Me}$]ZnOH with $[H(OEt_2)_2][B(Ar_F)_4]$ resulted in the formation of the zinc fluoride complex [Tp$^{Bu^t,Me}$]ZnF[19] as a result of decomposition of the $[B(Ar_F)_4]$ ligand.[20] In an effort to eliminate this decomposition pathway, we investigated the use of $[H(mesitylene)_2][B(C_6F_5)_4]$[21] in which the fluorinated substituents are perfluorophenyl rather than trifluoromethyl. However, this acid also resulted in decomposition.[22]

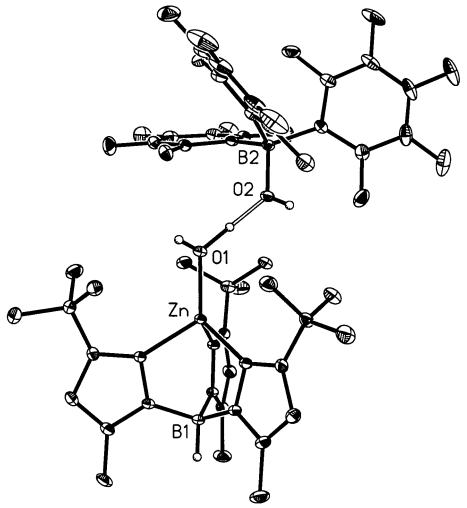

Figure 2. Molecular structure of {[Tp$^{Bu^t,Me}$]Zn(OH$_2$)}[HOB(C$_6$F$_5$)$_3$].

As a result of the failures employing $[H(OEt_2)_2][B(Ar_F)_4]$ and $[H(mesitylene)_2][B(C_6F_5)_4]$, alternative Brønsted acids were sought to effect protonation of [Tp$^{Bu^t,Me}$]ZnOH. Our attention turned to the aqua complex $(C_6F_5)_3B(OH_2)$ for several reasons. Firstly, $(C_6F_5)_3B(OH_2)$ is a strong Brønsted acid with a strength comparable to that of HCl in MeCN.[23] Secondly, we envisioned that steric interactions would inhibit the conjugate base $[(C_6F_5)_3BOH]^-$ from displacing the aqua ligand. Indeed, we discovered that $(C_6F_5)_3B(OH_2)$ is capable of protonating the hydroxide ligand of [Tp$^{Bu^t,Me}$]ZnOH to give an aqua complex {[Tp$^{Bu^t,Me}$]Zn(OH$_2$)}[HOB(C$_6$F$_5$)$_3$] in which the water molecule is *not* displaced by the counterion (Scheme 3), a result that has been previously communicated.[7] The importance of employing the $[(C_6F_5)_3BOH]^-$ counterion to stabilize the zinc aqua moiety is underscored by the fact that the coordinated water is readily displaced by addition of $[Bu_4^nN][I]$ to give [Tp$^{Bu^t,Me}$]ZnI (Scheme 3).[24]

The formation of $\{[Tp^{Bu^t,Me}]Zn(OH_2)\}^+$ is, as expected, reversible, and subsequent treatment with Et_3N regenerates [Tp$^{Bu^t,Me}$]ZnOH (Scheme 3). Furthermore, ^{1}H NMR spectroscopic studies of a solution of [Tp$^{Bu^t,Me}$]ZnOH, to which less than 1 equiv of $(C_6F_5)_3B(OH_2)$ has been added, indicate that proton transfer between [Tp$^{Bu^t,Me}$]ZnOH and {[Tp$^{Bu^t,Me}$]Zn-(OH$_2$)}[HOB(C$_6$F$_5$)$_3$] is rapid on the NMR time-scale.

The molecular structure of {[Tp$^{Bu^t,Me}$]Zn(OH$_2$)}[HOB(C$_6$F$_5$)$_3$] has been determined by X-ray diffraction, as illustrated in Figure 2; selected bond lengths are summarized in Table 1. Of particular note, the Zn−O bond [1.937(2) Å] is significantly

(18) (a) Hartmann, U.; Vahrenkamp, H. *Chem. Ber.* **1994**, *127*, 2381−2385. (b) Ruf, M.; Weis, K.; Vahrenkamp, H. *J. Chem. Soc., Chem. Commun.* **1994**, 135−136. (c) Brandsch, T.; Schell, F. A.; Weis, K.; Ruf, M.; Müller, B.; Vahrenkamp, H. *Chem. Ber.-Recueil* **1997**, *130*, 283−289. (d) Ruf, M.; Weis, K.; Brasack, I.; Vahrenkamp, H. *Inorg. Chim. Acta* **1996**, *250*, 271−281. (e) Ruf, M.; Weis, K.; Vahrenkamp, H. *Inorg. Chem.* **1997**, *36*, 2130−2137. (f) Hikichi, S.; Tanaka, M.; Moro-oka, Y.; Kitajima, N. *J. Chem. Soc., Chem. Commun.* **1992**, 814−815.

(19) (a) Kläui, W.; Schilde, U.; Schmidt, M. *Inorg. Chem.* **1997**, *36*, 1598−1601. (b) The ^{1}H NMR spectroscopic data for [Tp$^{Bu^t,Me}$]ZnF reported in the literature are incorrect due to an error in the solvent reference (Kläui, W., personal communication).

(20) Such decomposition is possibly a result of dissociation of water from the zinc center in $\{[Tp^{Bu^t,Me}]Zn(OH_2)\}^+$ creating a species with a highly electrophilic center $\{[Tp^{Bu^t,Me}]Zn\}^+$ that abstracts fluoride from the ligand.

(21) Reed, C. A.; Fackler, N. L. P.; Kim, K. C.; Stasko, D.; Evans, D. R.; Boyd, P. D. W.; Rickard, C. E. F. *J. Am. Chem. Soc.* **1999**, *121*, 6314−6315.

(22) It is possible that the decomposition which results from treatment of [Tp$^{Bu^t,Me}$]ZnOH with such acids is a result of reactivity at the B−H group. See, for example: Bergquist, C.; Koutcher, L.; Vaught, A. L.; Parkin, G. *Inorg. Chem.* **2002**, *41*, 625−627.

(23) Bergquist, C.; Bridgewater, B. M.; Harlan, C. J.; Norton, J. R.; Friesner, R. A.; Parkin, G. *J. Am. Chem. Soc.* **2000**, *122*, 10581−10590.

(24) [Tp$^{Bu^t,Me}$]ZnI has been previously described. See: Looney, A. Ph.D. Thesis, Columbia University, 1993.

Scheme 3

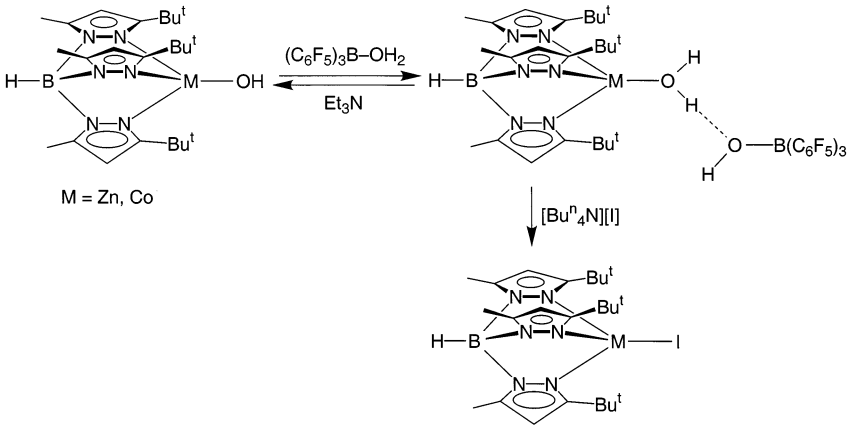

Table 1. Selected Bond Lengths (Å) and Angles (deg) for $\{[Tp^{Bu^t,Me}]M(OH_2)\}[HOB(C_6F_5)_3]$

	$\{[Tp^{Bu^t,Me}]Zn(OH_2)\}^+$ $[HOB(C_6F_5)_3]^-$	$\{[Tp^{Bu^t,Me}]Co(OH_2)\}^+$ $[HOB(C_6F_5)_3]^-$
M−O/Å	1.937(2)	1.963(2)
M−N/Å	2.007(2), 2.023(2), 2.025(2)	2.005(2), 2.016(2), 2.031(2)
O(1)···O(2)/Å	2.480(3)	2.498(2)
B−O/Å	1.502(3)	1.495(3)
O−M−N/deg	119.16(9), 119.87(9), 123.01(8)	118.37(8), 119.55(8), 123.39(8)

Table 2. Comparison of Zn−O and O···O Bond Lengths in Hydroxide and Aqua Complexes

	d(Zn–O)/Å	*d*(O···O)/Å	ref
Zn−OH			
$[Tp^{Bu^t,Me}]ZnOH$	1.85		*a*
$[Tp^{Cum,Me}]ZnOH$	1.85		*b*
$\{[Pim^{Bu^t,Pr^i}]ZnOH\}^+$	1.86		*c*
$[\{[12]aneN_3\}Zn(OH)]^+$	1.94		*d*
$\{[\eta^4\text{-}N\{CH_2CH_2NC(O)NHBu^t\}_3]ZnOH\}^{2-}$	2.02		*e*
$Zn-OH_2$			
$\{\{[Tp^{Cum,Me}]Zn\}_2(H_3O_2)\}^+$	1.87	2.40	*f*
$\{\{[Tp^{3-Py,Me}]Zn\}_2(H_3O_2)\cdot H_2O\}^+$	1.87, 1.92	2.45	*f*
$\{\{[Tp^{6-MePy,Me}]Zn\}_2(H_3O_2)\}^+$	1.87, 1.89	2.42	*f*
$\{\{[Tp^{Ph,Me}]Zn\}_2(H_3O_2)\}^+$	1.90	2.41	*g*
$\{[Tp^{Bu^t,Me}]Zn(OH_2)\}[HOB(C_6F_5)_3]$	1.94	2.48	this work
$[(X_6Et_3Imet_3)Zn(OH_2)\cdot(OH_2)]^{2+}$	1.97	2.54	*h*
$[(2\text{-}NH_2,5\text{-}EtSC_2N_2)_3Zn(OH)_2]^{2+}$	1.98		*i*
$\{[N(CH_2bimH)_3]Zn(OH)_2\}^{2+}$	2.01		*j*
$\{[MeC(O)S\}_3Zn(OH_2)\}^-$	2.08		*k*

[a] Alsfasser, R.; Trofimenko, S.; Looney, A.; Parkin, G.; Vahrenkamp, H. *Inorg. Chem.* **1991**, *30*, 4098−4100. [b] Ruf, M.; Vahrenkamp, H. *Inorg. Chem.* **1996**, *35*, 6571−6578. [c] Kimblin, C.; Allen, W. E.; Parkin, G. *J. Chem. Soc., Chem. Commun.* **1995**, 1813−1815. [d] Kimura, E.; Shiota, T.; Koike, T.; Shiro, M.; Kodama, M. *J. Am. Chem. Soc.* **1990**, *112*, 5805−5811. [e] MacBeth, C. E.; Hammes, B. S.; Young, V. G.; Borovik, A. S. *Inorg. Chem.* **2001**, *40*, 4733−4741. [f] Ruf, M.; Weis, K.; Vahrenkamp, H. *J. Am. Chem. Soc.* **1996**, *118*, 9288−9294. [g] Puerta, D. T.; Cohen, S. M. *Inorg. Chim. Acta* **2002**, *337*, 459−462. [h] Sénèque, O.; Rager, M.-N.; Giorgi, M.; Reinaud, O. *J. Am. Chem. Soc.* **2001**, *123*, 8442−8443. [i] Ishankhodzhaeva, M. M.; Umarov, B. B.; Kadyrova, Sh. A.; Parpiev, N. A.; Makhkamov, K. K.; Talipov, S. A. *Russ. J. Gen. Chem.* **2000**, *70*, 1113−1119. [j] (a) Ichikawa, K.; Nakata, K.; Ibrahim, M. M.; Kawabata, S. *Stud. Surf. Sci. Catal.* **1998**, *114*, 309−314. (b) Brandsch, T.; Schell, F. A.; Weis, K.; Ruf, M.; Muller, B.; Vahrenkamp, H. *Chem. Ber.-Recueil* **1997**, *130*, 283−289. [k] Sampanthar, J. T.; Deivaraj, T. C.; Vittal, J. J.; Dean, P. A. W. *J. Chem. Soc., Dalton Trans.* **1999**, 4419−4423.

longer than that in the parent hydroxide $[Tp^{Bu^t,Me}]ZnOH$ [1.850(8) Å],[8] in accord with the fact that the hydroxide ligand has been protonated. Correspondingly, the Zn−O bond length in $\{[Tp^{Bu^t,Me}]Zn(OH_2)\}^+$ is longer than the values in dinuclear $\{[Tp^{RR'}]Zn\}$ complexes with bridging $[H_3O_2]$ moieties [1.872(6)−1.916(6) Å],[25,26] as summarized in Table 2. The Zn−O bond length in $\{[Tp^{Bu^t,Me}]Zn(OH_2)\}^+$ is, however, slightly shorter than that in the aqua complex $[(X_6Et_3Imet_3)Zn(OH_2)\cdot(OH_2)]^{2+}$ [1.972(4) Å].[11] It is also interesting to note that the Zn−OH_2 bond length in $\{[Tp^{Bu^t,Me}]Zn(OH_2)\}[HOB(C_6F_5)_3]$ is actually shorter than that of the Zn−OH bond length [2.024(2) Å] in $\{[\eta^4\text{-}N\{CH_2CH_2NC(O)NHBu^t\}_3]ZnOH\}^{2-}$.[17] This discrepancy is a consequence of the Zn−O bond of $\{[\eta^4\text{-}N\{CH_2CH_2NC(O)NHBu^t\}_3]ZnOH\}^{2-}$ being exceptionally long for a hydroxide derivative; thus, as mentioned above for the cobalt counterpart, the long Zn−O bond length in $\{[\eta^4\text{-}N\{CH_2CH_2NC(O)NHBu^t\}_3]ZnOH\}^{2-}$ is presumably a result of the (i) zinc center being five-coordinate and anionic, and (ii) the hydroxide oxygen being a hydrogen bond receptor for two of the urea substituents.[17]

While the Zn−O bond is lengthened upon protonation, the B−O bond [1.502(3) Å] is substantially shortened upon deprotonation relative to that in the aqua complex $(C_6F_5)_3B(OH_2)$ [1.597(2) Å][27] and its various derivatives (Table 3); indeed, the B−O bond length in $\{[Tp^{Bu^t,Me}]Zn(OH_2)\}[HOB(C_6F_5)_3]$ is comparable to that in the $[(C_6F_5)_3BOH]^-$ anion (1.49 Å), as illustrated by $[Cp_2{*}Ta(Me)(OH)][(C_6F_5)_3BOH]$ and $[Et_3NH][(C_6F_5)_3BOH]$ (Table 3).

The structural study also indicates that the aqua complex $\{[Tp^{Bu^t,Me}]Zn(OH_2)\}^+$ exhibits a hydrogen bond interaction with the $[(C_6F_5)_3BOH]^-$ anion, characterized by an O···O separation of 2.480(3) Å. As such, $\{[Tp^{Bu^t,Me}]Zn(OH_2)\}[HOB(C_6F_5)_3]$ may be viewed formally as a derivative of the $[H_3O_2]^-$ anion, of which structurally related derivatives include $\{\{[Tp^{RR'}]Zn\}_2(H_3O_2)\}^+$ and $\{[(C_6F_5)_3B]_2(H_3O_2)\}^-$ (Tables 2 and 3). However, it is important to note that the $[H_3O_2]^-$ moiety of $\{[Tp^{Bu^t,Me}]Zn(OH_2)\}[HOB(C_6F_5)_3]$ is asymmetric, such that the zinc aqua description of the structure is meaningful; thus, the bridging hydrogen is displaced from the center towards the zinc oxygen rather than towards the boron oxygen [O(1)−H(3) = 1.09(4) Å and O(2)−H(3) = 1.39(4) Å]. Asymmetry of this magnitude is not observed for the aforementioned $\{\{[Tp^{RR'}]Zn\}_2(H_3O_2)\}^+$ derivatives. For example, the bridging hydrogen in $\{\{[Tp^{Ph,Me}]Zn\}_2(H_3O_2)\}^+$ is symmetrically located between the two oxygen atoms with O−H distance of 1.21 Å.[26] As such, an "aqua" formulation is not particularly appropriate for $\{\{[Tp^{Ph,Me}]Zn\}_2$-

(25) Ruf, M.; Weis, K.; Vahrenkamp, H. *J. Am. Chem. Soc.* **1996**, *118*, 9288−9294.
(26) Puerta, D. T.; Cohen, S. M. *Inorg. Chim. Acta* **2002**, *337*, 459−462.
(27) Doerrer, L. H.; Green, M. L. H. *J. Chem. Soc., Dalton Trans.* **1999**, 4325−4329.

Table 3. Comparison of B−O and O···O Bond Lengths in Hydroxide and Aqua Complexes

	d(B–O)/Å	*d*(O···O)/Å	ref
B−OH_2			
$(C_6F_5)_3B(OH_2)$	1.60		*a*
$(C_6F_5)_3B(OH_2)$·dioxane·CH_2Cl_2	1.57		*b*
$[(C_6F_5)_3B(OH_2)]$·$2H_2O$	1.58		*c*
$(C_6F_5)_3B(OH_2)$·HOBu^t	1.58		*d*
B(μ-OH)			
{[Tp$^{Bu^t,Me}$]Zn(OH_2)}[$HOB(C_6F_5)_3$]	1.50	2.48	this work
{[$(C_6F_5)_3B(OH_2)$][$HOB(C_6F_5)_3$]}$^-$	1.51, 1.53	2.41	*e*
(Bu$^t_2$bpy)Pt(Me){[$HOB(C_6F_5)_3$]}	1.53		*f*
[CpIr(COD)H][{$(C_6F_5)_3B$}$_2$(μ-OH)]	1.56, 1.57		*c*
B−OH			
[Cp$_2$*Ta(Me)(OH)][$(C_6F_5)_3BOH$]	1.49		*g*
[Et_3NH][$(C_6F_5)_3BOH$]	1.49		*h*

[a] Doerrer, L. H.; Green, M. L. H. *J. Chem. Soc., Dalton Trans.* **1999**, 4325−4329. [b] Janiak, C.; Braun, L.; Scharmann, T. G.; Girgsdies, F. *Acta Crystallogr.* **1998**, *C54*, 1722−1724. [c] Danopoulos, A. A.; Galsworthy, J. R.; Green, M. L. H.; Cafferkey, S.; Doerrer, L. H.; Hursthouse, M. B. *Chem. Commun.* **1998**, 2529−2530. [d] Bergquist, C.; Bridgewater, B. M.; Harlan, C. J.; Norton, J. R.; Friesner, R. A.; Parkin, G. *J. Am. Chem. Soc.* **2000**, *122*, 10581−10590. [e] Drewitt, M. J.; Niedermann, M.; Baird, M. C. *Inorg. Chim. Acta* **2002**, *340*, 207−210. [f] Hill, G. S.; Manojlovic-Muir, L.; Muir, K. W.; Puddephatt, R. J. *Organometallics* **1997**, *16*, 525−530. [g] Schaefer, W. P.; Quan, R. W.; Bercaw, J. E. *Acta Crystallogr.* **1993**, *C49*, 878−881. [h] Siedle, A. R.; Newmark, R. A.; Lamanna, W. M.; Huffman, J. C. *Organometallics* **1993**, *12*, 1491−1492. Note that the B−O bond length for [Et_3NH][$(C_6F_5)_3BOH$] in this paper is erroneously attributed to [Et_3NH][$(C_6H_5)_3BOH$] due to a typographic error (Huffman, J. C., personal communication).

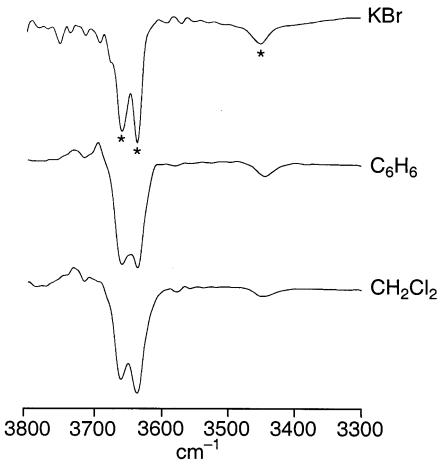

Figure 3. IR spectra of {[Tp$^{Bu^t,Me}$]Zn(OH_2)}[$HOB(C_6F_5)_3$] in (a) KBr, (b) C_6H_6 solution, and (c) CH_2Cl_2 solution. The similarity of the three spectra indicates that the hydrogen bonding interaction observed in the solid state is retained in C_6H_6 and CH_2Cl_2 solution.

Table 4. ν(O−H) IR Stretching Frequencies (cm^{-1}) of {[Tp$^{Bu^t,Me}$]MOH_2}[$HOB(C_6F_5)_3$] in KBr Pellets

{[Tp$^{Bu^t,Me}$]ZnOH_2}[$HOB(C_6F_5)_3$]	{[Tp$^{Bu^t,Me}$]CoOH_2}[$HOB(C_6F_5)_3$]
3662	3666
3641	3637
3450	3423

$(H_3O_2)\}^+$. In addition, the Zn−O distance is in accord with this notion; that is, the Zn−O bond in {{[Tp^{Ph,Me}]Zn}$_2$(H_3O_2)}$^+$ [1.895(1) Å] is shorter than that in {[Tp$^{Bu^t,Me}$]Zn(OH_2)}[HOB-$(C_6F_5)_3$] [1.937(2) Å] and is only slightly longer than that in [Tp$^{RR'}$]ZnOH hydroxide derivatives (1.85 Å).[28] Furthermore, as compared to $(C_6F_5)_3B(OH_2)$, the B−O bond of {[Tp$^{Bu^t,Me}$]Zn-(OH_2)}[$HOB(C_6F_5)_3$] is short [1.502(3) Å] (Table 3), which is also consistent with the description that the bridging proton resides principally on the zinc bound oxygen atom.

In view of the difficulty of isolating a {[Tp$^{RR'}$]Zn(OH_2)}$^+$ derivative with other counterions, it is evident that it is the ability of $[(C_6F_5)_3BOH]^-$ to serve as a hydrogen bond acceptor that provides the critical stabilizing factor which allows for the successful isolation of {[Tp$^{Bu^t,Me}$]Zn(OH_2)}[$HOB(C_6F_5)_3$]. The hydrogen bonding interaction of the zinc aqua ligand is also notable because it bears analogies to the active site in carbonic anhydrase. Specifically, the zinc water ligand at the active site of carbonic anhydrase also participates in a hydrogen bond with Thr-199.[29,30] This interaction has been shown to be important to the functioning of the enzyme, with Thr-199 having been described as a "doorkeeper" that helps to block the displacement of the aqua ligand by certain inhibitors that cannot form a hydrogen bond.[30] In addition to the interaction with Thr-199, the zinc-bound water of carbonic anhydrase is also part of a hydrogen bonding network involving additional water molecules which mediate as a proton shuttle to His-64, prior to proton transfer to the surrounding medium.[31]

IR spectroscopic studies, illustrated in Figure 3, demonstrate that the hydrogen bonding interaction in {[Tp$^{Bu^t,Me}$]Zn(OH_2)}-[$HOB(C_6F_5)_3$] also persists in solution. In the solid state, the [H_3O_2] moiety is characterized by ν_{OH} absorptions at 3662, 3641, and 3450 cm^{-1} in the IR spectrum, of which the lowest energy signal is attributed to the hydrogen bonded interaction. These ν_{OH} absorptions are virtually unperturbed in both benzene and dichloromethane solution (Figure 3 and Table 4), consistent with the hydrogen bond being retained in solution. The persistence of the hydrogen bonding interaction in solution is in accord with the notion that O···O separations that are less than 2.50 Å are often classified as "very strong".

However, despite the fact that the hydrogen bond in {[Tp$^{Bu^t,Me}$]-Zn(OH_2)}[$HOB(C_6F_5)_3$] persists in benzene and dichloromethane solution, IR spectroscopy indicates that it is not retained in either tetrahydrofuran or acetonitrile solution. Thus, rather than exhibiting the three band pattern associated with the [H_3O_2] moiety illustrated in Figure 3, the IR spectrum of {[Tp$^{Bu^t,Me}$]-Zn(OH_2)}[$HOB(C_6F_5)_3$] in either THF or MeCN possesses two bands that are identical to those of a solution of water in the respective solvent (Figure 4). This observation suggests that the donor solvent disrupts the hydrogen bond between cation and anion, allowing the aqua ligand to be displaced by a solvent molecule, and thereby forming {[Tp$^{Bu^t,Me}$]Zn(L)}$^+$ or a subsequent derivative. In support of this suggestion, the related cationic zinc pyridine complex {[Tp^{Cum,Me}]Zn(NC_5H_5)}[ClO_4] has been structurally characterized.[18c]

(28) Furthermore, the O···O distance in {{[Tp^{Ph,Me}]Zn}$_2$(H_3O_2)}$^+$ (2.41 Å) is shorter than that in {[Tp$^{Bu^t,Me}$]Zn(OH_2)}[$HOB(C_6F_5)_3$] (2.48 Å), consistent with a stronger hydrogen bond in the former complex.
(29) The O···O distance is 2.7 Å. See ref 30.
(30) Liljas, A.; Håkansson, K.; Jonsson, B. H.; Xue, Y. *Eur. J. Biochem.* **1994**, *219*, 1−10.
(31) (a) Denisov, V. P.; Jonsson, B.-H.; Halle, B. *J. Am. Chem. Soc.* **1999**, *121*, 2327−2328. (b) Toba, S.; Colombo, G.; Merz, K. M., Jr. *J. Am. Chem. Soc.* **1999**, *121*, 2290−2302. (c) Christianson, D. W.; Fierke, C. A. *Acc. Chem. Res.* **1996**, *29*, 331−339 and references therein. (d) Liang, Z.; Xue, Y.; Behravan, G.; Jonsson, B.-H.; Lindskog, S. *Eur. J. Biochem.* **1993**, *211*, 821−827. (e) Merz, K. M., Jr. *J. Mol. Biol.* **1990**, *214*, 799−802. (f) Eriksson, A. E.; Jones, A. T.; Liljas, A. *Proteins* **1988**, *4*, 274−282. (g) Xue, Y.; Liljas, A.; Jonsson, B.-H.; Lindskog, S. *Proteins* **1993**, *17*, 93−106. (h) Håkansson, K.; Carlsson, M.; Svensson, L. A.; Liljas, A. *J. Mol. Biol.* **1992**, *227*, 1192−1204. (i) Smedarchina, Z.; Siebrand, W.; Fernández-Ramos, A.; Cui, Q. *J. Am. Chem. Soc.* **2003**, *125*, 243−251.

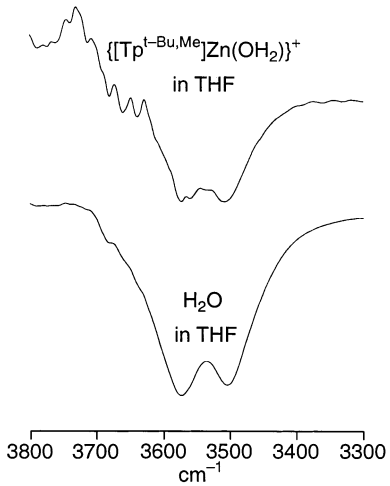

Figure 4. IR spectra of (a) $\{[Tp^{But,Me}]Zn(OH_2)\}[HOB(C_6F_5)_3]$ and (b) H_2O in THF solution. The similarity of the two spectra indicates that the THF has caused the zinc aqua ligand to be displaced.

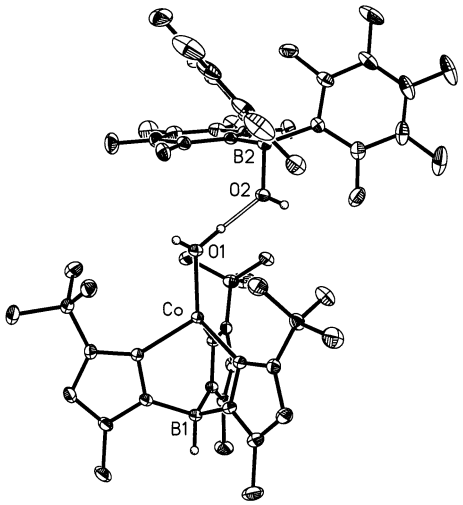

Figure 5. Molecular structure of $\{[Tp^{But,Me}]Co(OH_2)\}[HOB(C_6F_5)_3]$.

In addition to studying the protonation of $[Tp^{But,Me}]$ZnOH, we have also investigated the interaction of the cobalt hydroxide $[Tp^{But,Me}]$CoOH with $(C_6F_5)_3B(OH_2)$ to give the aqua complex $\{[Tp^{But,Me}]Co(OH_2)\}[HOB(C_6F_5)_3]$ (Scheme 3), which has been structurally characterized by X-ray diffraction, as illustrated in Figure 5. Selected bond lengths for $\{[Tp^{But,Me}]Co(OH_2)\}[HOB(C_6F_5)_3]$ are compared to those of the zinc analogue in Table 1, thereby indicating that the structural features are similar. Furthermore, comparison between the structures of $[Tp^{But,Me}]$CoOH and $\{[Tp^{But,Me}]Co(OH_2)\}[HOB(C_6F_5)_3]$ indicate that protonation results in geometrical changes similar to those observed for the zinc system. Specifically, (i) the Co−O bond length in the aqua cation $\{[Tp^{But,Me}]Co(OH_2)\}^+$ [1.963(2) Å] is longer than that in the hydroxide $[Tp^{But,Me}]$CoOH [1.859(3) Å],[32] and (ii) the B−O bond of the anion [1.495(3) Å] is shorter than that in $(C_6F_5)_3B(OH_2)$ [1.597(2) Å]. There is also a hydrogen bond between the cobalt aqua and the boron hydroxide ligands, with an O···O separation of 2.498(2) Å. In addition to the structural similarity between $\{[Tp^{But,Me}]Zn(OH_2)\}[HOB(C_6F_5)_3]$ and $\{[Tp^{But,Me}]Co(OH_2)\}[HOB(C_6F_5)_3]$, they also exhibit similar reactivity towards deprotonation and displacement of the $[(C_6F_5)_3BOH]^-$ anion. Thus, the cobalt complex is deprotonated by Et_3N to regenerate $[Tp^{But,Me}]$CoOH and reacts with $[Bu_4^nN][I]$ to give $[Tp^{But,Me}]$CoI (Scheme 3).

Table 5. Selected Bond Lengths (Å) for Geometry Optimized [Tp]MOH, $\{[Tp]M(OH_2)\}^+$, and $\{[Tp]M(OH_2)\}[HOBF_3]$ (M = Zn, Co), with Values for Co in Parentheses

	[Tp]MOH	$\{[Tp]M(OH_2)\}[HOBF_3]$	$\{[Tp]M(OH_2)\}^+$
d(M−O)	1.863 (1.812)	1.944 (1.930)	2.072 (2.061)
d(M−N_{av})	2.145 (2.103)	2.099 (2.052)	2.056 (2.014)
d(MO−μH)		1.189 (1.087)	
d(BO−μH)		1.214 (1.378)	
d(O···O)		2.389 (2.436)	

(c) DFT Geometry Optimization Calculations on [Tp]MOH and $\{[Tp]M(OH_2)\}^+$ Derivatives (M = Zn, Co). To complement the experimental study and provide information pertaining to the structural changes involved in protonation of a zinc hydroxide ligand, we have performed DFT (B3LYP) calculations on the model species [Tp]ZnOH and $\{[Tp]Zn(OH_2)\}^+$. The geometry optimized structures of these complexes are illustrated in Figure 6.[33] Importantly, the zinc coordination geometry calculated for [Tp]ZnOH (Table 5) corresponds very closely to the experimental structure of $[Tp^{But,Me}]$ZnOH. Thus, the Zn−OH bond length calculated for [Tp]ZnOH [1.863 Å] is virtually identical to that for the experimental structure of $[Tp^{But,Me}]$ZnOH [1.850(8) Å];[8] likewise, the calculated (2.15 Å) and experimental (2.10 Å)[8] average Zn−N bond lengths are very similar. The good correlation between the experimental and calculated structures is a clear indication of the reliability of the calculations.

Comparison of the calculated structures of [Tp]ZnOH and $\{[Tp]Zn(OH_2)\}^+$ indicates that protonation of the hydroxide ligand lengthens the Zn−O bond in $[TpZn(OH_2)]^+$ substantially to 2.072 Å, while shortening the average Zn−N bond length [2.06 Å], as summarized in Table 5. Both of these changes are reflected in the experimental structures of $[Tp^{But,Me}]$ZnOH and $\{[Tp^{But,Me}]Zn(OH_2)\}^+$. Specifically, the Zn−O bond of $[Tp^{But,Me}]$ZnOH increases to 1.973 Å upon formation of $\{[Tp^{But,Me}]Zn(OH_2)\}^+$, while the average Zn−N bond length decreases to 2.02 Å. The lengthening of the Zn−O bond upon protonation is merely a consequence of the fact that the aqua ligand is coordinated by a dative covalent bond (L) rather than a normal covalent bond (X).[34] On the other hand, the shortening of the Zn−N bond is a result of the fact that dative L bonds are particularly sensitive to the charge on a metal center; thus, as a $[L_2X]$ ligand,[34] the Zn−N bonds are shortened upon formation of a cation.

Although the calculations reproduce the overall coordination changes at the zinc center upon protonation, it is evident that the lengthening of the Zn−O bond in $\{[Tp^{But,Me}]Zn(OH_2)\}^+$ is not as large as that predicted for $[TpZn(OH_2)]^+$. Since a possible explanation for this difference resides with the fact that the $\{[Tp^{But,Me}]Zn(OH_2)\}^+$ is involved in the aforementioned hydrogen bonding interaction with the $[B(C_6F_5)_3BOH]^-$ counterion, we addressed this possibility by performing a DFT calculation on the hypothetical species $\{[Tp]Zn(OH_2)\}[HOBF_3]$.

(32) For further comparison, the Co−O bond lengths in the five-coordinate complexes $\{[P(CH_2CH_2PPh_2)_3]CoOH\}^+$ and $\{[P(CH_2CH_2PPh_2)_3]Co(OH_2)\}^{2+}$ are 1.873(7) and 2.102(6) Å, respectively. See ref 16.

(33) For other calculations of $[Tp^{RR'}]$ZnOH derivatives, see: Bergquist, C.; Storrie, H.; Koutcher, L.; Bridgewater, B. M.; Friesner, R. A.; Parkin, G. *J. Am. Chem. Soc.* **2000**, *122*, 12651−12658.

(34) For the $[L_lX_x]$ classification of ligands, see: Green, M. L. H. *J. Organomet. Chem.* **1995**, *500*, 127−148.

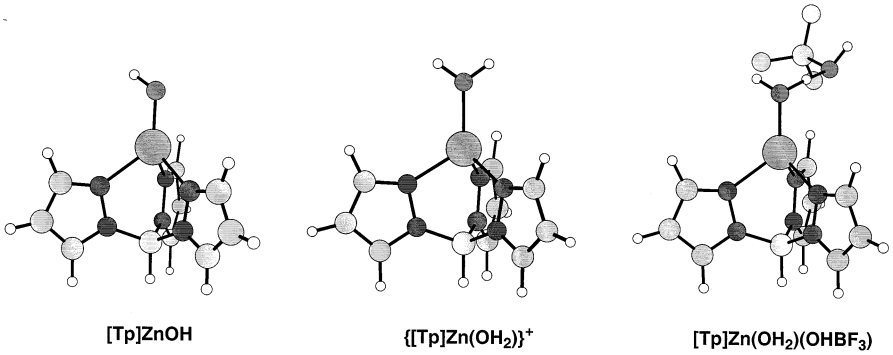

Figure 6. DFT (B3LYP) geometry optimized structures of [Tp]ZnOH, $\{[Tp]Zn(OH_2)\}^+$, and $\{[Tp]Zn(OH_2)\}[HOBF_3]$.

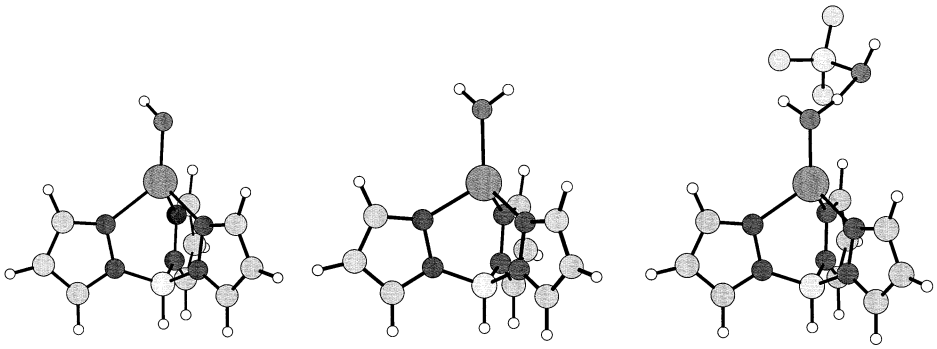

Figure 7. DFT (B3LYP) geometry optimized structures of [Tp]CoOH, $\{[Tp]Co(OH_2)\}^+$, and $\{[Tp]Co(OH_2)\}[HOBF_3]$.

Significantly, the Zn−O (1.944 Å) bond length in $\{[Tp]Zn(OH_2)\}[HOBF_3]$ is reduced from that of the free cation $\{[Tp]Zn(OH_2)\}^+$ and is comparable to the experimental value in $\{[Tp^{Bu^t,Me}]Zn(OH_2)\}[HOB(C_6F_5)_3]$ [1.937(2) Å].

We have also performed geometry optimization calculations on the analogous cobalt complexes, [Tp]CoOH, $\{[Tp]Co(OH_2)\}^+$, and $\{[Tp]Co(OH_2)\}[HOBF_3]$, as illustrated in Figure 7 and Table 5.[35] Comparison with the zinc counterparts indicates that the respective structures are similar, with the principal difference being that the Co−X bonds are only marginally shorter than the corresponding Zn−X bonds in each case (Table 5), in line with the difference in the radii of Co (1.243 Å) and Zn (1.295 Å).[36]

(d) Comparison of the Acidity of $\{[Tp^{RR'}]Zn(OH_2)\}^+$ and $\{[Tp^{RR'}]Co(OH_2)\}^+$. The existence of the hydrogen bonding interactions in $\{[Tp^{Bu^t,Me}]M(OH_2)\}[HOB(C_6F_5)_3]$ (M = Zn, Co) is a clear indication of the acidic nature of the coordinated water molecule in the $\{[Tp^{Bu^t,Me}]M(OH_2)\}^+$ cations. In this regard, it is important to note that an early important issue concerned with the mechanism of action of carbonic anhydrase centered on the simple question of whether it is possible for a zinc-bound water molecule to have a pK_a as low as 7 to enable it to be sufficiently deprotonated at neutral pH to play a catalytically important role.[37] However, studies on model species and calculations indicate that the pK_a is dictated strongly by the coordination number and charge of the complex, with the pK_a decreasing with decreasing coordination number and increasing positive charge on the metal center.[5] On the basis of these studies, the low pK_a associated with the coordinated water at the active site of carbonic anhydrase is, today, not considered unreasonable.

However, it is also recognized that the catalytic properties of carbonic anhydrase are not only influenced by the pK_a of the metal bound water molecule, but also by the pK_a of a histidine residue in the vicinity of the active site (His-64 for bovine CAII and His-64 or His-200 for CAI), which serves as a shuttle to transfer a metal aqua proton to the reaction medium.[38] The protonation state of this histidine residue also influences the pK_a of the coordinated water, and Bertini has performed a spectroscopic study on Co^{II}−CA to extract the pK_a values for deprotonation of $[Co^{II}(OH_2)]\cdots$(His) and $[Co^{II}(OH_2)]\cdots(His-H^+)$ species.[39] The results indicate that the pK_a for deprotonation of the water in $[Co^{II}(OH_2)]\cdots(His-H^+)$ is considerably less than that for $[Co^{II}(OH_2)]\cdots$(His). For example, the pK_a values of $[Co^{II}(OH_2)]\cdots(His-H^+)$ and $[Co^{II}(OH_2)]\cdots$(His) for Co^{II} bovine carbonic anhydrase II are 6.1 and 7.6, respectively,[39a] while the pK_a value for deprotonation of the histidine residue in $[Co^{II}(OH_2)]\cdots(His-H^+)$ is intermediate, with a value of 6.3.[40]

In view of the fact that two ionizing groups are involved in the catalysis, i.e., $M^{II}-OH_2$ and $His-H^+$, analysis of the activity

(35) While tetrahedral cobalt(II) complexes are usually high spin (quartet), Peters has recently reported an interesting example of a pseudotetrahedral low spin Co(II) complex, namely $[PhB(CH_2PPh_2)_3]CoI$ [Jenkins, D. M.; Di Bilio, A. J.; Allen, M. J.; Betley, T. A.; Peters, J. C. *J. Am. Chem. Soc.* **2002**, *124*, 15336−15350]. To establish that the cobalt(II) complexes [Tp]CoOH and $\{[Tp]Co(OH_2)\}^+$ are high spin, calculations were also performed on the doublet states. The calculation indicated that, in each case, the high spin state is more stable.

(36) These values are the effective radii of the metal atoms in diatomic MH. See: Pauling, L. *The Nature of The Chemical Bond*, 3rd ed.; Cornell University Press: Ithaca, NY, 1960; p 257.

(37) Wooley, P. *Nature* **1975**, *258*, 677−682.

(38) Lindskog, S. In *Metal Ions in Biology*; Spiro, T. G., Ed.; Wiley: New York, 1983; Vol. 5, p 77.

(39) (a) Bertini, I.; Dei, A.; Luchinat, C.; Monnanni, R. *Inorg. Chem.* **1985**, *24*, 301−303. (b) Bertini, I.; Luchinat, C.; Scozzafava, A. *Inorg. Chim. Acta* **1980**, *46*, 85−89.

(40) For Co^{II} human carbonic anhydrase I, the pK_a values are: $[Co^{II}(OH_2)]\cdots(His-H^+)$, 7.1; $[Co^{II}(OH_2)]\cdots$(His), 8.4; and $[Co^{II}(OH_2)]\cdots(His-H^+)$, 7.2.

in terms of a single apparent acid dissociation constant is problematic in terms of interpretation. For example, a comparative activity study of Zn^{II} and Co^{II} bovine carbonic anhydrase has identified that the pK_a associated with a single apparent acid dissociation constant is smaller for the Co^{II} enzyme (6.6) than that for the Zn^{II} enzyme (6.9) when determined by consideration of the pH profile of k_{cat}; however, the pK_a is larger for the Co^{II} enzyme (7.2) than that for the Zn^{II} enzyme (7.0) when determined by consideration of the pH profile of k_{cat}/K_M.[41,42] In this regard, it has been commented upon that predictions of the pK_a difference between cobalt and zinc complexes have been hampered by a lack of systematic studies as a function of coordination geometry and ligand environment.[2] It is, therefore, worthwhile to determine exactly how the pK_a of an aqua ligand in a well-defined tetrahedral $\{[N_3]M^{II}(OH_2)\}$ complex depends on whether the metal is zinc or cobalt.

The isolation of $\{[Tp^{But,Me}]Zn(OH_2)\}[HOB(C_6F_5)_3]$ and $\{[Tp^{But,Me}]Co(OH_2)\}[HOB(C_6F_5)_3]$ provides a system that should enable the determination of how substitution of zinc by cobalt influences the pK_a of the coordinated water in synthetic analogues of carbonic anhydrase. However, in view of the complications described above concerning the role of noninnocent counteranions, pK_a studies of this type are nontrivial (especially in aqueous solution).[43] Nevertheless, we have demonstrated that $\{[Tp^{But,Me}]Zn(OH_2)\}[HOB(C_6F_5)_3]$ is readily deprotonated by Et_3N (Scheme 1) and measurement of this equilibrium constant would readily yield the pK_a of $\{[Tp^{But,Me}]Zn(OH_2)\}^+$ since the pK_a of $[Et_3NH]^+$ is known. However, the equilibrium constant for deprotonation of $\{[Tp^{But,Me}]Zn(OH_2)\}^+$ by Et_3N is sufficiently great that it is immeasurable; as such, we can only demonstrate that the pK_a of $\{[Tp^{But,Me}]Zn(OH_2)\}^+$ is considerably less than that of $[Et_3NH]^+$, i.e., 10.72 in aqueous solution.[44] Likewise, the equilibrium constant for protonation of $[Tp^{But,Me}]ZnOH$ by $(C_6F_5)_3B(OH_2)$ is sufficiently great that it indicates that the pK_a of $\{[Tp^{But,Me}]Zn(OH_2)\}^+$ is considerably greater than that of $(C_6F_5)_3B(OH_2)$, which has been estimated to be less than ca. 0.9 in aqueous solution.[23] Neither of these experiments, therefore, is capable of determining the pK_a of $\{[Tp^{But,Me}]Zn(OH_2)\}^+$, although they indicate that it lies in the rather unsatisfactorily large range of 0.9−10.7.[45] For a routine pK_a determination, this would simply mean that a different acid or base should be chosen to determine the equilibrium constant. However, as discussed above, the zinc aqua ligand is readily displaced by anions, so the choice of suitable acids and bases is severely limited. Therefore, we have performed DFT calculations to determine how the metal center influences the pK_a of the zinc and cobalt aqua complexes, $\{[Tp]Zn(OH_2)\}^+$ and $\{[Tp]Co(OH_2)\}^+$.[46]

Table 6. Calculated Energetics for the Deprotonation of $\{[Tp]M(OH_2)\}^+$ (M = Zn, Co)

	$\Delta H^{SCF(g)}$ kcal mol^{-1} [a]	ΔH^{ZPE} kcal mol^{-1} [b]	ΔH^{T} kcal mol^{-1} [b]	$\Delta H_{25°C}^{(g)}$ kcal mol^{-1} [b]
Zn	244.97	−7.83	−0.50	236.63
Co	244.25	−8.00	−0.46	235.78
	$\Delta S_{25°C}$ cal mol^{-1} K^{-1}	$\Delta G_{25°C}^{(g)}$ kcal mol^{-1}	$\Delta H_{solv\ correct}$ kcal mol^{-1} [c]	$\Delta G_{25°C}^{(solv)}$ kcal mol^{-1} [d]
Zn	−3.89	237.79	42.09	279.88
Co	−3.33	236.78	44.15	280.93

[a] $\Delta H^{SCF(g)}$ is the gas-phase electronic enthalpy change determined using DFT (B3LYP) calculations with cc-pVTZ(-f) (H, B, C, N, O), LACV3P** (Co), and LAV3P** (Zn) basis sets. [b] $\Delta H_{25°C}^{(g)}$ is the sum of three terms: $\Delta H^{SCF(g)}$, the electronic enthalpy in the gas phase; ΔH^{ZPE}, the enthalpy correction due to zero point energy differences; and ΔH^{T}, the enthalpy correction due to thermal excitation. [c] $\Delta H_{solv\ correct}$ is determined using the Jaguar Poisson−Boltzmann solver, with the dielectric constant set to a value of 78.54 for water at 25 °C. [d] $\Delta G_{25°C}^{(solv)} = \Delta G_{25°C}^{(g)} + \Delta H_{solv\ correct}$.

The gas-phase deprotonation enthalpies of $\{[Tp]Zn(OH_2)\}^+$ and $\{[Tp]Co(OH_2)\}^+$ were calculated at the B3LYP level using cc-pVTZ(-f) (H, B, C, N, O, F), LACV3P** (Co), and LAV3P** (Zn) basis sets, as summarized in Table 6. The free energy for deprotonation of $\{[Tp]Zn(OH_2)\}^+$ and $\{[Tp]Co(OH_2)\}^+$ in the gas phase was determined from $\Delta H^{SCF(g)}$ by taking into account (i) enthalpy corrections due to zero point energy differences (ΔH^{ZPE}), (ii) enthalpy corrections due to thermal excitation (ΔH^{T}), and (iii) entropic differences. Finally, a correction for solvation ($\Delta H_{solv\ correct}$) using a continuum dielectric solvation model to approximate an aqueous medium was obtained using the Jaguar Poisson−Boltzmann solver, with the dielectric constant set to a value of 78.54 for water at 25 °C.[47] These calculations indicate that the solution free energies of deprotonation of $\{[Tp]Zn(OH_2)\}^+$ and $\{[Tp]Co(OH_2)\}^+$ are comparable, with that for the cobalt complex being only 1.05 kcal mol^{-1} more endothermic (i.e., less acidic). The difference in $\Delta G_{25\ °C}^{(solv)}$ values corresponds to a modest pK_a difference of 0.77 units. The calculations thus indicate that the pK_a values of $\{[Tp]Zn(OH_2)\}^+$ and $\{[Tp]Co(OH_2)\}^+$ are comparable, a result that is in line with the aforementioned reports of the aqua ligand of Co^{II}−carbonic anhydrase being both slightly more and slightly less acidic than that of the zinc enzyme. The similarity of the calculated pK_a values of $\{[Tp]Zn(OH_2)\}^+$ and $\{[Tp]Co(OH_2)\}^+$ is also in accord with the observation that Co^{II} is a successful substitute for Zn^{II} in carbonic anhydrase.[2,3,15]

(e) Comparison of the Reactivity of $[Tp^{But,Me}]MOH$ and $\{[Tp^{But,Me}]M(OH_2)\}[HOB(C_6F_5)_3]$ towards CO_2 (M = Zn, Co). An important notion of the proposed mechanism of action of carbonic anhydrase (Scheme 1) is that the coordinated water is deprotonated prior to reaction with CO_2.[1,48] However, such a proposal has not been demonstrated by direct comparison of the reactivity of a pair of structurally characterized tetrahedral

(41) Kogut, K. A.; Rowlett, R. S. *J. Biol. Chem.* **1987**, *262*, 16417−16424.
(42) For further discussion concerned with pK_a differences pertaining to other forms of carbonic anhydrase, see: (a) Alber, B. E.; Colangelo, C. M.; Dong, J.; Stålhandske, C. M. V.; Baird, T. T.; Tu, C.; Fierke, C. A.; Silverman, D. N.; Scott, R. A.; Ferry, J. G. *Biochemistry* **1999**, *38*, 13119−13128. (b) Elleby, B.; Chirica, L. C.; Tu, C.; Zeppezauer, M.; Lindskog, S. *Eur. J. Biochem.* **2001**, *268*, 1613−1619. (c) Moratal, J. M.; Martinez-Ferrer, M. J.; Donaire, A.; Aznar, L. *J. Inorg. Biochem.* **1992**, *45*, 65−71.
(43) For efforts to determine comparative pK_a values for zinc and cobalt aqua complexes in carbonic anhydrase synthetic analogues, see: (a) Koerner, T. B.; Brown, R. S. *Can. J. Chem.* **2002**, *80*, 183−191. (b) Jairam, R.; Potvin, P. G. *J. Org. Chem.* **1992**, *57*, 4136−4141. (c) Brown, R. S.; Salmon, D.; Curtis, N. J.; Kusuma, S. *J. Am. Chem. Soc.* **1982**, *104*, 3188−3194. (d) Brown, R. S.; Zamkanei, M. *Inorg. Chim. Acta* **1985**, *108*, 201−207.
(44) Dean, J. A. *Lange's Handbook of Chemistry*, 13th ed.; McGraw-Hill: New York, 1972; p 5−58.
(45) It should be noted that an estimate of ca. 6.5 has been cited for the pK_a of $\{[Tp^{But,Me}]Zn(OH_2)\}^+$, although specific details of the experiment to determine this value were not provided. See ref 6b.
(46) For other calculations on zinc and cobalt species with relevance to carbonic anhydrase, see: (a) Garmer, D. R.; Krauss, M. *J. Am. Chem. Soc.* **1992**, *114*, 6487−6493. (b) Garmer, D. R.; Krauss, M. *Int. J. Quantum Chem.* **1992**, *42*, 1469−1477. (c) Sola, M.; Mestres, J.; Duran, M.; Carbo, R. *J. Chem. Inf. Comput. Sci.* **1994**, *34*, 1047−1053. (d) Vedani, A.; Huhta, D. W. *J. Am. Chem. Soc.* **1990**, *112*, 4759−4767.
(47) For a review of such models, see: Tomasi, J.; Persico, M. *Chem. Rev.* **1994**, *94*, 2027−2094.
(48) Zhang, X.; Hubbard, C. D.; van Eldik, R. *J. Phys. Chem.* **1996**, *100*, 9161−9171.

Scheme 4

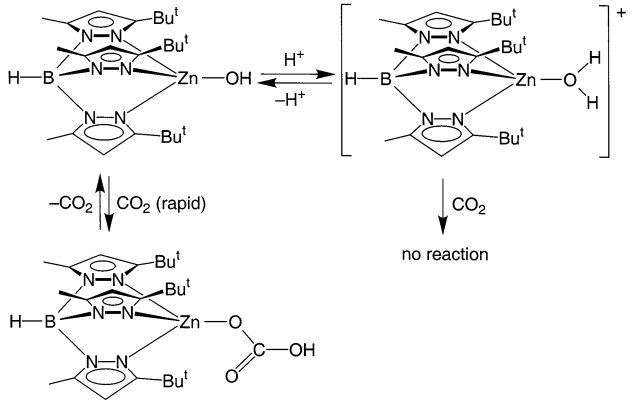

Scheme 5

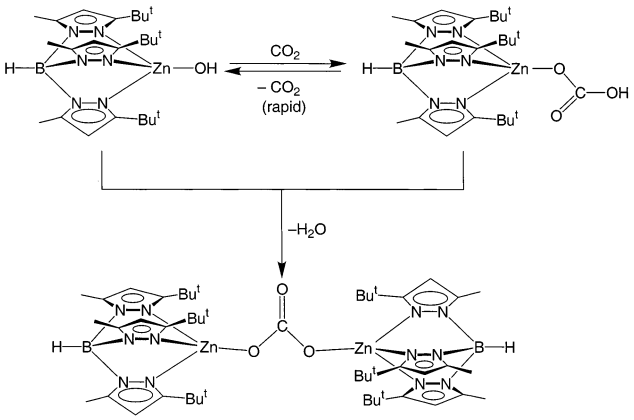

{[N_3]Zn(OH)} and {[N_3]Zn(OH_2)}$^+$ complexes with coordination environments that mimic well the active site of carbonic anhydrase. The isolation of both [$Tp^{But,Me}$]ZnOH and its conjugate acid {[$Tp^{But,Me}$]Zn(OH_2)}[$HOB(C_6F_5)_3$], therefore, provides a unique opportunity to study such a proposition in a well-defined system.

We have previously demonstrated that, in the presence of CO_2, [$Tp^{But,Me}$]ZnOH is in rapid equilibrium with the bicarbonate derivative [$Tp^{But,Me}$]ZnOC(O)OH (Scheme 4).[49] As a result of the facile interconversion between [$Tp^{But,Me}$]Zn(OCO_2H) and [$Tp^{But,Me}$]ZnOH, condensation of the latter two molecules generates a bridging carbonate complex {[$Tp^{But,Me}$]Zn}$_2$(μ-η^1,η^1-CO_3) which may be isolated over a period of days by virtue of its lower solubility (Scheme 5). The bridging carbonate complex {[$Tp^{But,Me}$]Zn}$_2$(μ-η^1,η^1-CO_3) is, however, extremely sensitive towards water, thereby regenerating the hydroxide derivative [$Tp^{But,Me}$]ZnOH.[49]

In contrast to the facile reaction of [$Tp^{But,Me}$]ZnOH with CO_2, its conjugate acid {[$Tp^{But,Me}$]Zn(OH_2)}[$HOB(C_6F_5)_3$] does *not* react with CO_2 under comparable conditions (Scheme 4). Since lifetime broadening is not observed for {[$Tp^{But,Me}$]Zn(OH_2)}$^+$ in the presence of CO_2, we can estimate that its reactivity towards CO_2 is at least a factor of 10^2 less than that of [$Tp^{But,Me}$]-ZnOH. Such direct comparison provides an excellent demonstration that deprotonation of the zinc bound water is indeed an essential step in the mechanism of action of carbonic anhydrase.

The cobalt hydroxide complex [$Tp^{But,Me}$]CoOH also reacts with CO_2 to form a bridging carbonate complex {[$Tp^{But,Me}$]Co}$_2$-

(49) Looney, A.; Han, R.; McNeill, K.; Parkin, G. *J. Am. Chem. Soc.* **1993**, *115*, 4690−4697.

Scheme 6

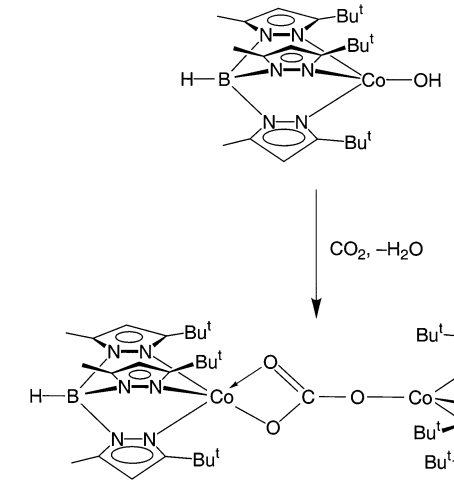

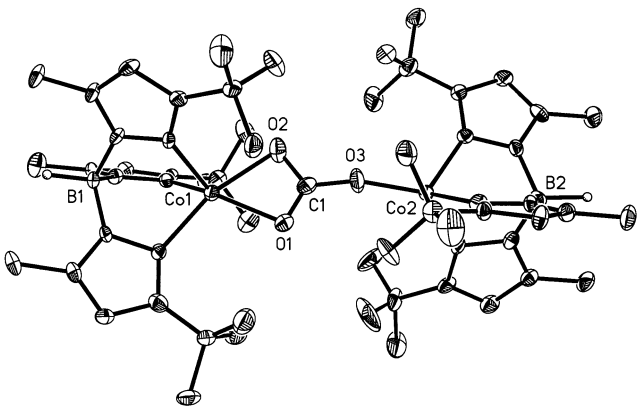

Figure 8. Molecular structure of {[$Tp^{But,Me}$]Co}$_2$(μ-η^1,η^2-CO_3). Selected bond lengths (Å) and angles (deg): Co(1)−O(1), 2.035(5); Co(1)−O(2), 2.117(5); Co(2)−O(3), 1.836(6); C(1)−O(3)−Co(2) 163.9(6).

(μ-η^1,η^2-CO_3), presumably via the initial formation of a bicarbonate derivative (Scheme 6). As described above for the zinc system, the cobalt aqua complex {[$Tp^{But,Me}$]Co(OH_2)}-[$HOB(C_6F_5)_3$] does *not* react with CO_2 under comparable conditions, providing a further example which indicates that prior deprotonation is essential for promoting reactivity towards CO_2.

An interesting difference between the zinc and cobalt systems pertains to the coordination mode of the bridging carbonate ligands. Thus, whereas the carbonate ligand of the zinc complex {[$Tp^{But,Me}$]Zn}$_2$(μ-η^1,η^1-CO_3) bridges in a unidentate manner to each zinc center, an X-ray diffraction study demonstrates that the carbonate ligand in the cobalt counterpart {[$Tp^{But,Me}$]Co}$_2$-(μ-η^1,η^2-CO_3) is unidentate to one cobalt center and bidentate to the other (Figure 8). The Co−O bond length associated with the unidentate interaction is 1.836(6) Å, while those associated with the bidentate component are 2.035(5) and 2.117(5) Å.

The difference in the coordination geometries of {[$Tp^{But,Me}$]-Zn}$_2$(μ-η^1,η^1-CO_3) and {[$Tp^{But,Me}$]Co}$_2$(μ-η^1,η^2-CO_3) provides an illustration of how Co^{II} promotes bidentate coordination as compared to that of zinc. This observation is of significance in light of the proposition that bidentate coordination of a bicarbonate ligand could inhibit its displacement and thereby reduce the efficiency of carbonic anhydrase catalytic cycle,[49,50] a suggestion that is consistent with the facts that Co^{II}−carbonic anhydrase is less active than the zinc enzyme and that the

bicarbonate ligand in the Co^{II} derivative coordinates in a bidentate fashion.[3h,51] It should be recognized, however, that the extrapolation to the enzyme system is not perfect because the carbonate ligands in the zinc and cobalt complexes bridge two metals, whereas the bicarbonate ligand in carbonic anhydrase coordinates to only a single metal. Nevertheless, the structures of $\{[Tp^{But,Me}]Zn\}_2(\mu\text{-}\eta^1,\eta^1\text{-}CO_3)$ and $\{[Tp^{But,Me}]Co\}_2(\mu\text{-}\eta^1,\eta^2\text{-}CO_3)$ are still in accord with the general notion that cobalt favors bidentate coordination to a greater extent than does zinc in coordination environments analogous to the active site of carbonic anhydrase.

In addition to comparison with the zinc complex, $\{[Tp^{But,Me}]Zn\}_2(\mu\text{-}\eta^1,\eta^1\text{-}CO_3)$, it is worthwhile to compare the carbonate coordination mode of $\{[Tp^{But,Me}]Co\}_2(\mu\text{-}\eta^1,\eta^2\text{-}CO_3)$ with that of $\{[Tp^{Pri_2}]Co\}_2(\mu\text{-}\eta^2,\eta^2\text{-}CO_3)$,[13] which features less sterically demanding isopropyl substituents in the 3-position of the pyrazolyl rings. As a result of the reduced steric demands, the carbonate ligand in $\{[Tp^{Pr_2{}^i}]Co\}_2(\mu\text{-}\eta^2,\eta^2\text{-}CO_3)$ coordinates to *both* cobalt centers in a bidentate manner with Co−O bond lengths in the range 1.99−2.27 Å.

Conclusion

In summary, protonation of the zinc hydroxide complex $[Tp^{But,Me}]ZnOH$ by $(C_6F_5)_3B(OH_2)$ yields the aqua derivative $\{[Tp^{But,Me}]Zn(OH_2)\}[HOB(C_6F_5)_3]$, a transformation that results in a lengthening of the Zn−O bond by ca. 0.1 Å. The protonation is reversible, and treatment of $\{[Tp^{But,Me}]Zn(OH_2)\}^+$ with Et_3N regenerates $[Tp^{But,Me}]ZnOH$. Consistent with the notion that the catalytic hydration of CO_2 by carbonic anhydrase requires deprotonation of the coordinated water molecule, $\{[Tp^{But,Me}]Zn(OH_2)\}^+$ is inert towards CO_2, whereas $[Tp^{But,Me}]ZnOH$ is in rapid equilibrium with the bicarbonate complex $[Tp^{But,Me}]ZnOC(O)OH$. The cobalt hydroxide $[Tp^{But,Me}]CoOH$ is likewise protonated by $(C_6F_5)_3B(OH_2)$ to yield the aqua derivative $\{[Tp^{But,Me}]Co(OH_2)\}[HOB(C_6F_5)_3]$, which is isostructural with the zinc complex. X-ray diffraction studies demonstrate the existence of a hydrogen bonding interaction between the zinc (and cobalt) aqua and boron hydroxide moieties. This hydrogen bonding interaction may be viewed as providing an analogy to that between the aqua ligand and Thr-199 at the active site of carbonic anhydrase.

The similarities between the zinc and cobalt systems, in terms of both (i) the molecular structures of the hydroxide $[Tp^{But,Me}]MOH$ and aqua $\{[Tp^{But,Me}]M(OH_2)\}^+$ complexes, and (ii) the calculated pK_a values of $\{[Tp]Zn(OH_2)\}^+$ and $\{[Tp]Co(OH_2)\}^+$, are in accord with the observation that Co^{II} is a successful substitute for Zn^{II} in carbonic anhydrase. In this regard, the different coordination modes adopted by the carbonate complexes, $\{[Tp^{But,Me}]Zn\}_2(\mu\text{-}\eta^1,\eta^1\text{-}CO_3)$ and $\{[Tp^{But,Me}]Co\}_2(\mu\text{-}\eta^1,\eta^2\text{-}CO_3)$, concur with the suggestion that a possible reason for the lower activity of Co^{II}−carbonic anhydrase is associated with the enhanced bidentate coordination of bicarbonate to Co^{II} which inhibits its displacement.

Experimental Section

General Considerations. Unless otherwise noted, all reactions and manipulations were performed under an Ar or N_2 atmosphere employing standard Schlenk and glovebox techniques. NMR spectra were recorded on Bruker Avance 300 DRX, Bruker Avance 300 DRX, Bruker Avance 400 DRX, and Bruker Avance 500 DMX spectrometers. ^1H and ^{13}C chemical shifts are reported in ppm relative to $SiMe_4$ ($\delta = 0$) and were referenced internally with respect to the protio solvent impurity ($\delta =$ 7.15 for C_6D_5H) and the ^{13}C resonances ($\delta = 128.0$ for C_6D_6), respectively. ^{19}F NMR spectra were measured on a Bruker Avance 300 DRX spectrometer and were referenced relative to $CFCl_3$ ($\delta = 0.00$) using external $PhCF_3$ ($\delta = -63.72$) as a calibrant.[52] All coupling constants are reported in Hz. IR spectra were recorded as KBr pellets or as a solution between KBr plates on a Perkin-Elmer Spectrum 2000 spectrophotometer and are reported in cm^{-1}. C, H, and N elemental analyses were measured using a Perkin-Elmer 2400 CHN Elemental Analyzer. $[Tp^{But,Me}]ZnOH$,[8] $[Tp^{But,Me}]CoOH$,[14] and $(C_6F_5)_3B(OH_2)$[23] were prepared by literature methods.

Synthesis of $\{[Tp^{But,Me}]Zn(OH_2)\}[HOB(C_6F_5)_3]$. A solution of $(C_6F_5)_3B(OH_2)$ (144 mg, 0.27 mmol) in C_6H_6 (4 mL) was added dropwise to a solution of $[Tp^{But,Me}]ZnOH$ (137 mg, 0.27 mmol) in C_6H_6 (8 mL). The solution was concentrated, filtered, and allowed to crystallize at room temperature, giving $\{[Tp^{But,Me}]Zn(OH_2)\}[HOB(C_6F_5)_3]\cdot 0.5(C_6H_6)$ as a white solid (222 mg, 77%). Anal. Calcd for $C_{45}H_{46}B_2F_{15}N_6O_2Zn$: C, 50.3; H, 4.3; N, 7.8. Found: C, 50.2; H, 4.1; N, 8.2. ^1H NMR (C_6D_6): 1.15 [s, 3(C(CH_3)$_3$)], 1.89 [s, 3(CH_3)], 5.42 [s, 3(C_3N_2H)], *H*B and *H*O were not observed. ^{13}C NMR (C_6D_6): 12.4 [q, $^1J_{C-H} = 128$, 3(CH_3)], 30.2 [q, $^1J_{C-H} = 125$, 3(C(CH_3)$_3$)], 31.1 [s, 3(C(CH_3)$_3$)], 103.7 [d, $^1J_{C-H} = 178$, 3(C_3N_2H) (1C)], 145.5 [s, 3(C_3N_2H) (1C)], 163.3 [s, 3(C_3N_2H) (1C)]. ^{19}F NMR (C_6D_6): −136.0 [d, $^3J_{F-F} =$ 22, *ortho*], −165.0 [m, *meta*], −159.9 [t, $^3J_{F-F} = 21$, *para*]. IR (KBr, cm^{-1}): 3662 (m) [ν(O−H)], 3641 (m) [ν(O−H)], 3450 (m) [ν(O−H)], 2971 (m), 2565 (m) [ν(B−H)], 1644 (m), 1543 (m), 1517 (s), 1464 (vs), 1368 (m), 1280 (m), 1187 (m), 1088 (s), 1033 (w), 976 (s), 922 (m), 895 (m), 810 (m), 767 (m), 683 (m). IR (C_6H_6, cm^{-1}): 3660 (m) [ν(O−H)], 3637 (m) [ν(O−H)], 3445 (m) [ν(O−H)]. IR (CH_2Cl_2, cm^{-1}): 3662 (m) [ν(O−H)], 3638 (m) [ν(O−H)], 3449 (vw) [ν(O−H)].

Synthesis of $\{[Tp^{But,Me}]Co(OH_2)\}[HOB(C_6F_5)_3]$. A solution of $(C_6F_5)_3B(OH_2)$ (117 mg, 0.22 mmol) in C_6H_6 (3 mL) was added dropwise to a purple solution of $[Tp^{But,Me}]CoOH$ (110 mg, 0.22 mmol) in C_6H_6 (10 mL), resulting in the formation of a dark blue solution. The solution was stirred for 1 h at room temperature, concentrated to 3 mL, filtered, and allowed to crystallize at room temperature, giving $\{[Tp^{But,Me}]Co(OH_2)\}[HOB(C_6F_5)_3]\cdot 0.5(C_6H_6)$ as a blue solid (110 mg, 47%). Anal. Calcd for $C_{45}H_{46}B_2F_{15}N_6O_2Co$: C, 50.3; H, 4.3; N, 7.8. Found: C, 50.5; H, 3.4; N, 7.8. ^1H NMR (C_6D_6): 4.8 [br, 3(C(CH_3)$_3$)], 21.0 [br, 3(CH_3)], 80.8 [br, 3(C_3N_2H)], *H*B and *H*O were not observed. ^{19}F NMR (C_6D_6): −125.5 [br, *ortho*], −165.3 [br, *meta*], −160.1 [m, *para*]. IR (KBr, cm^{-1}): 3666 (m) [ν(O−H)], 3637 (m) [ν(O−H)], 3423 (vw) [ν(O−H)], 2971 (m), 2565 (w) [ν(B−H)], 1644 (m), 1542 (m), 1517 (s), 1464 (vs), 1366 (m), 1279 (m), 1244 (w), 1185 (m), 1087 (s), 1066 (m), 1034 (w), 976 (s), 927 (m), 895 (w), 811 (m), 764 (m), 683 (w), 648 (w). IR (C_6H_6, cm^{-1}): 3665 (m) [ν(O−H)], 3633 (m) [ν(O−H)], 3451 (w) [ν(O−H)]. IR (CH_2Cl_2, cm^{-1}): 3666 (m) [ν(O−H)], 3633 (m) [ν(O−H)], 3451 (vw) [ν(O−H)].

Reaction of $[Tp^{But,Me}]ZnOH$ with $[(3,5\text{-}(CF_3)_2C_6H_3)_4B][H(OEt_2)_2]$. A solution of $[Tp^{But,Me}]ZnOH$ (7 mg, 0.01 mmol) in $CDCl_3$ (ca 0.6 mL) was treated with a solution of $[(3,5\text{-}(CF_3)_2C_6H_3)_4B][H(OEt_2)_2]$ in Et_2O (500 μL of 0.1 M). The reaction was monitored by ^1H NMR spectroscopy, thereby demonstrating the formation of $[Tp^{But,Me}]ZnF$.[19]

Reaction of $\{[Tp^{But,Me}]M(OH_2)\}[HOB(C_6F_5)_3]$ with CO_2. A solution of $\{[Tp^{But,Me}]M(OH_2)\}[HOB(C_6F_5)_3]$ (M = Co, Zn) in C_6D_6 was

(50) (a) Han, R.; Parkin, G. *J. Am. Chem. Soc.* **1991**, *113*, 9707−9708. (b) Han, R.; Looney, A.; McNeill, K.; Parkin, G.; Rheingold, A. L.; Haggerty, B. S. *J. Inorg. Biochem.* **1993**, *49*, 105−121. (c) Looney, A.; Saleh, A.; Zhang, Y.; Parkin, G. *Inorg. Chem.* **1994**, *33*, 1158−1164. (d) Kimblin, C.; Murphy, V. J.; Hascall, T.; Bridgewater, B. M.; Bonanno, J. B.; Parkin, G. *Inorg. Chem.* **2000**, *39*, 967−974.

(51) Furthermore, the metal center in Co^{II}−CA also adopts five-coordination with inhibitors such as HSO_3^- and NO_3^-, whereas that in Zn^{II}−CA retains tetrahedral coordination. See ref 30.

(52) Evans, B. J.; Doi, J. T.; Musker, W. K. *J. Org. Chem.* **1990**, *55*, 2337−2344.

Table 7. Crystal, Intensity Collection, and Refinement Data

	$[Tp^{Bu^t,Me}]CoOH$	$\{[Tp^{Bu^t,Me}]Co\}_2(\mu\text{-}\eta^1,\eta^2\text{-}CO_3)\cdot 2(C_6H_6)$	$\{[Tp^{Bu^t,Me}]ZnOH_2\}^+[HOB(C_6F_5)_3]^-\cdot 0.5(C_6H_6)$	$\{[Tp^{Bu^t,Me}]CoOH_2\}^+[HOB(C_6F_5)_3]^-\cdot 0.5(C_6H_6)$
lattice	monoclinic	monoclinic	monoclinic	monoclinic
formula	$C_{24}H_{38}BN_6O_6Co$	$C_{61}H_{92}B_2N_{12}O_3Co_2$	$C_{45}H_{46}B_2F_{15}N_6O_2Zn$	$C_{45}H_{46}B_2F_{15}N_6O_2Co$
formula weight	496.34	1180.95	1074.87	1068.43
space group	$P2_1/n$ (No. 14)	$P2_1/c$ (No. 14)	$P2_1/n$ (No. 14)	$P2_1/n$ (No. 14)
a/Å	9.5712(8)	19.096(3)	9.8138(7)	9.8536(11)
b/Å	30.523(2)	14.431(2)	33.873(3)	34.001(4)
c/Å	9.5763(7)	24.382(4)	14.7045(11)	14.7391(16)
α/deg	90	90	90	90
β/deg	100.910(1)	95.035(4)	94.4760(10)	94.502(3)
γ/deg	90	90	90	90
V/Å^3	2747.1(4)	6693(2)	4873.3(6)	4923(1)
Z	4	4	4	4
temp (K)	238	238	203	233
μ (Mo Kα), mm^{-1}	0.71073	0.71073	0.71073	0.71073
no. of data	6341	15 472	11 269	11 130
no. of params	314	730	669	669
R_1	0.0570	0.0766	0.0499	0.0468
wR_2	0.1237	0.0793	0.1015	0.1088
GOF	1.023	1.008	1.032	1.032

treated with CO_2 (1 atm) in a NMR tube. The sample was monitored by ^{1}H NMR spectroscopy, thereby indicating that no reaction occurred.

Reaction of $\{[Tp^{Bu^t,Me}]M(OH_2)\}[HOB(C_6F_5)_3]$ with Et_3N. A solution of $\{[Tp^{Bu^t,Me}]M(OH_2)\}[HOB(C_6F_5)_3]$ (M = Co, Zn) in C_6D_6 in a NMR tube was treated with Et_3N. The reaction was monitored by ^{1}H NMR spectroscopy, thereby demonstrating the clean formation of $[Tp^{Bu^t,Me}]MOH$.[8,14]

Reaction of $\{[Tp^{Bu^t,Me}]M(OH_2)\}[HOB(C_6F_5)_3]$ with $[Bu_4^nN][I]$. A solution of $\{[Tp^{Bu^t,Me}]M(OH_2)\}[HOB(C_6F_5)_3]$ (M = Co, Zn) in C_6D_6 was treated with $[Bu_4^nN][I]$. The reaction was monitored by ^{1}H NMR spectroscopy, thereby demonstrating the clean formation of $[Tp^{Bu^t,Me}]$-MI.[53]

Synthesis of $\{[Tp^{Bu^t,Me}]Co\}_2(\mu\text{-}\eta^1,\eta^2\text{-}CO_3)$. A purple solution of $[Tp^{Bu^t,Me}]CoOH$ (100 mg, 0.2 mmol) in benzene (3 mL) was treated with CO_2 (1 atm), resulting in the instantaneous formation of a blue solution of $\{[Tp^{Bu^t,Me}]Co\}_2(\mu\text{-}\eta^1,\eta^2\text{-}CO_3)$, in quantitative yield as judged by ^{1}H NMR spectroscopy. The volatile components were removed in vacuo, giving $\{[Tp^{Bu^t,Me}]Co\}_2(\mu\text{-}\eta^1,\eta^2\text{-}CO_3)$ as a blue solid (56 mg). ^{1}H NMR (C_6D_6): −5.4, 21.9, 65.2 (assignments not given due to paramagnetic nature of the sample).

X-ray Structure Determinations. X-ray diffraction data were collected on a Bruker P4 diffractometer equipped with a SMART CCD detector, and crystal data, data collection, and refinement parameters are summarized in Table 7. The structures were solved using direct methods and standard difference map techniques and were refined by full-matrix least-squares procedures on F^2 with SHELXTL (Version 6.10).[54] Hydrogen atoms on carbon were included in calculated positions.

(53) $[Tp^{Bu^t,Me}]ZnI^a$ and $[Tp^{Bu^t,Me}]CoI^b$ have been previously described. ^{1}H NMR spectrum of $[Tp^{Bu^t,Me}]ZnI$ (C_6D_6): 1.61 [s, 3(C(CH_3)$_3$)], 2.06 [s, 3(CH_3)], 5.65 [s, 3(C_3N_2H)], *H*B not observed. ^{1}H NMR spectrum of $[Tp^{Bu^t,Me}]CoI$ (C_6D_6): 8.3 [br, 3(C(CH_3)$_3$)], 15.6 [br, 3(CH_3)], 75.9 [br, 3(C_3N_2H)], −13.2 [br, *H*B]. (a) Reference 24. (b) Reference 14.

Computational Details. All calculations were carried out using DFT as implemented in the Jaguar 4.1 suite of ab initio quantum chemistry programs.[55] Geometry optimization and solvent corrections were performed with the B3LYP[56] functional employing 6-31G** (H, B, C, N, O, F), LACVP** (Co), and LAV3P** (Zn) basis sets.[57] The energies of the optimized structures were reevaluated by additional single point calculations on each optimized geometry using the cc-pVTZ(-f)[58] (H, B, C, N, O, F), LACV3P** (Co), and LAV3P** (Zn) basis sets.[57] Solvation energies were calculated using the Jaguar Poisson−Boltzmann solver, with the dielectric constant set to a value of 78.54 for water at 25 °C. Vibrational frequency calculations to derive zero point energy and entropy corrections were determined at the B3LYP level of theory using 6-31G**, LACVP**, and LAV3P** basis sets.

Acknowledgment. We thank the National Institutes of Health (Grant GM46502) for support of this research and Dr. Mu-Hyun Baik for helpful comments.

Supporting Information Available: Crystallographic CIF files. This material is available free of charge via the Internet at http://pubs.acs.org.

JA034711J

(54) Sheldrick, G. M. SHELXTL, An Integrated System for Solving, Refining and Displaying Crystal Structures from Diffraction Data; University of Göttingen: Göttingen, Federal Republic of Germany, 1981.
(55) Jaguar 4.1; Schrödinger, Inc.: Portland, Oregon, 2001.
(56) (a) Slater, J. C. *Quantum Theory of Molecules and Solids: The Self-Consistent Field for Molecules and Solids*; McGraw-Hill: New York, 1974; Vol. 4. (b) Vosko, S. H.; Wilk, L.; Nusair, M. *Can. J. Phys.* **1980**, *58*, 1200−1211. (c) Lee, C. T.; Yang, W. T.; Parr, R. G. *Phys. Rev. B* **1988**, *37*, 785−789. (d) Becke, A. D. *Phys. Rev. A* **1988**, *38*, 3098−3100. (e) Becke, A. D. *J. Chem. Phys.* **1993**, *98*, 5648−5652.
(57) (a) Hay, P. J.; Wadt, W. R. *J. Chem. Phys.* **1985**, *82*, 299−310. (b) Wadt, W. R.; Hay, P. J. *J. Chem. Phys.* **1985**, *82*, 284−298. (c) Hay, P. J.; Wadt, W. R *J. Chem. Phys.* **1985**, *82*, 270−283.
(58) Dunning, T. H. *J. Chem. Phys.* **1989**, *90*, 1007−1023.